A Comprehensive Anatomical Characterization and Radiographic Study of Stage III Testicular Cancer in a 31-Year-Old Male Patient

PROGRAM # LB104

***Jose L. Mas*[1A], *Ernest F. Talarico, Jr.*[1A], *and Jonathan A. Jones*[2B]**

[1]*Department of Anatomy & Cell Biology,* [2]*Department of Family Medicine,* [A]*Indiana University School of Medicine – Northwest (Gary, IN),* [B]*Union Hospital (Terre Haute, IN)*

ABSTRACT

Purpose: The purpose of this investigation was to characterize an unusual case of stage III testicular germ cell tumor (TGCT) in a 31-year-old male with metastases to nodes, bone, viscera and brain, and to understand all possible routes of metastatic disease. Testicular cancer (TC) has an increasing incidence worldwide, and its etiology, risk factors and pathogenesis are not completely understood.
Methods: Medical records were reviewed, and the cadaveric specimen evaluated by physical examination and gross dissection. Paraffin embedded tissue sections of the primary tumor were stained with Hematoxylin and Eosin (H&E) for histological study. To examine metastatic spread, pre- and post-mortem digital radiologic image acquisition was done using x-ray films, and high- resolution CT Scans and MRI Scans. Image analysis, multi-planar reformatting, and three-dimensional (3-D) reconstruction were done on radiographic series.
Results: Dissection showed masses bilaterally from the apex through the lung base; masses on the internal thoracic wall, and hepatomegaly and splenomegaly with multiple tumor masses. Testicular parenchyma was composed of primitive germ cells that formed glomeruloid or embryonal-like structures, as well as areas with a micro-cystic histologic pattern and areas of fibrous dysplasia. Medical imaging 3-D video radiographic dissection was notable for a 38.45 mm diameter, mid-brain tumor; extreme hepatomegaly with numerous tumors, a large penetrating tumor of the left ilium, and multiple tumors throughout both lungs and the thoracolumbar spine (T5-S1).
Conclusion: This study provides insight into the histology and metastatic spread of TGCT that is essential for clinicians to understand in the evaluation and treatment of TC patients.

INTRODUCTION

Testicular cancer (TC) is defined as a malignant neoplasm of the male sex organ (i.e., testicle). Although TC accounts for 1% of all male cancers (1, 2), it is the most common neoplasm among young men between 15-40 years of age (1-3). Approximately 98% of all TCs are testicular germ cell tumors (TGCTs) (3, 4), and are histologically classified as seminoma, embryonal carcinoma, yolk sack tumor (YST), teratoma or choriocarcinoma (5). Other types (i.e., non-TGCTs) include lymphomas, and those arising from Sertoli and Leydig cells. Among the TGCTs, the most interesting is the YST, which is the most common TC in infants and young children (6). In adults, this pure form of tumor is rare; instead, yolk sack elements frequently occur in combination with embryonal carcinoma making detection of adult YST difficult. However, recent studies linking the production of alpha-fetoprotein (AFP) with the presence of YST elements within a tumor complex demonstrate that AFP is a very useful marker for the presence of YST and emphasizes the importance of recognition and detection of elements (7).

Over the past 40 years, the incidence of TGCTs in developed countries has steadily risen (1, 4, 8). Male Scandinavians have the highest incidence of TC worldwide (3, 4). Even further, the incidence of TGCTs in the U.S. is notably higher among Caucasian men than any other ethnicity (9). Incidence rates are very low in Asia and Africa. Current studies indicate that TGCT incidence is increasing most rapidly among U.S. Hispanic males (10) with a peak incidence between ages of 20-40 years.

Research has suggested risk factors that include genetics, familial incidence, environment, recreational drug use, occupation, increased height and HIV/AIDs (9). However, cryptorchidism is the most well characterized risk factor for TC (11), and TC is 10-40 fold higher in cryptorchid testes. It is estimated that 12% of all TGCTs arise in cryptorchid testes (11). In recent years, genetic disorders such as mutations of loci on chromosome 12q21 have been identified and suggested to be associated with TGCTs (9, 12, 13).

The most common site for TC metastasis is the lymph nodes in the abdomen, but metastasis to the lung, liver, bones and brain can also occur (14, 15). This suggests multiple metastatic routes including hematogenous, lymphatic and direct invasion. Men with brain metastases (BM), have a poor overall survival (14). Even further, because BM of TGCTs are rare, the best method for medical management remains uncertain (15). The survivors of TC are at risk of reoccurrence and a range of other disorders (9). Thus, because of the aggressiveness of TGCTs and their increasing incidence, a more comprehensive understanding of TGCTs is needed to so that clinicians can better diagnose, treat and manage patients.

The present report investigates the unusual case of a 31-year-old male with stage III TGCT and metastases to nodes, bone, viscera and a large brain tumor, while utilizing imaging technology to better characterize this disorder.

CORRESPONDENCE

Jose L. Mas, D.V.M.
Assistant Professor of Clinical Anatomy & Cell Biology
Indiana University School of Medicine - Northwest
Dunes Medical Professional Building, Room 3058, 3400 Broadway
Gary, Indiana 46408-1197 USA
TEL: 219-981-5625; FAX: 219-980-6566; Email: jlmas@iun.edu

METHODS

Cadaveric Specimen. This study was conducted on a 31-year-old male cadaver with consent of this anatomical donor's family and with authorization of the State of Indiana Anatomical Education Program. Medical and hospital records and tissue slides/blocks of the donor were acquired. Secondary medical history was obtained through structured interviews with the maternal parent.

Gross Examination and Photography. Detailed physical examination was performed utilizing a "donor report" (i.e., similar to an autopsy report), where gross observations and quantitative data were collected. Digital photography of the external features and viscera was done using a NIKON D3100 SLR Camera (B&H Foto & Electronic Corporation, NY) equipped with an 18-55 mm VR NIKKOR Macro lens and a Nikon 40 mm f/2.8G AF-S DX NIKKOR 2200 VR Micro lens.

X-Ray Film Imaging. Plain x-ray imaging was performed and the following plain films were obtained: (1) anterior-posterior (AP) chest (CXR); (2) AP abdominopelvic; (3) upper extremity (pectoral girdle, brachium, antebrachium and carpus/manus); (4) lower extremity (pelvic girdle, thigh, leg and foot); (5) AP skull and lateral (Lat) skull.

Advanced Medical Imaging. Full-body, high-resolution CT and MRI imaging was completed using a 64-slice CT scanner (General Electric Lightspeed® capable of 3-D reconstruction, and an MRI scanner (General Electric HIGH Speed MRI). Coronal (COR), axial (AX) and sagittal (SAG) views were generated both digitally and on film. Additional MRI scans included: (a) MRI of the brain including T1-weighted (Wtd) axial and sagittal; T2-Wtd AX, AX diffusion, and FLAIR axial scans; (b) MRI of the abdomen and pelvis to include T1- and T2-Wtd sequences in COR and AX planes; (c) MRI of the knees, hips, and shoulders to consist of T1-, T2-Wtd, and STIR images in at least two planes; (d) MRI of the entire spine including T1- and T2-Wtd SAG images.

Image Analysis. Processing of images, creations of 3D-reconstructions, and quantitative image analysis were done using Konica PDI Viewer 1.00 V1.0R0.00 (KONICA Minolta, Ramsey, NJ) and TDK CDRS Dashboard V1.0.0.5 (TDK Medical, Minneapolis, MN) for digital x-ray films; eFILMTM Lite™ Viewer 3.0 (Merge Healthcare, Chicago, IL) for radiographic series from CT-Scans; and Philips iSite Viewer (Philips iSite, Amsterdam, Netherlands) for radiographic series from MRI Scans. Additional image analysis and reconstruction-reformatting was done using PACSGEAR (Perceptive Software, Pleasanton, CA) on radiographic series from CT scans and MRI scans. Multi-planar reformatting was used to view slices in different planes for further analysis and measurement.

Video Clips. BodyViz® Interactive Anatomy Software Version 5.0 (Clive, IA) was used with Digital Imaging and Communications in Medicine (DICOM) data files from CT and MRI scans of the patient to construct high-resolution, 3-D images and video clips, as well as freeze-frame images. Tumor masses were measured and analyzed using video clips.

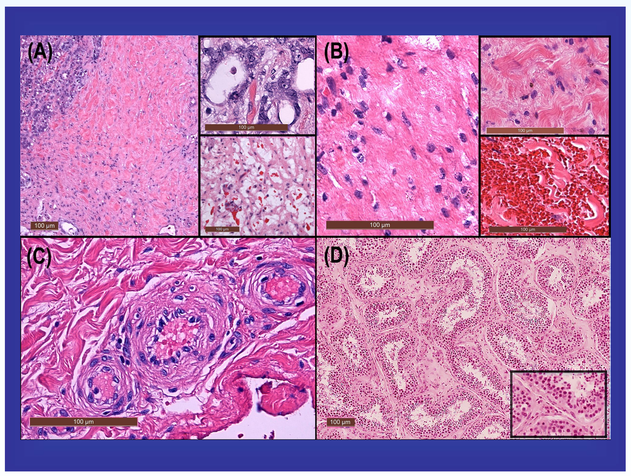

Figure 1. Histology of Testicular Tissue. (A) Survey view showing total lack of normal testicular parenchyma; with inset of glomeruloid (above) or embryonal-like structures and micro-cystic pattern (below). **(B)** Multiple areas of fibrous dysplasia without evidence of normal testicular parenchyma; with insets of higher-magnification fibrosis (above) and hemorrhagic area (below). **(C)** Schiller-Duval bodies are distinctive perivascular structures seen in the YST. Each consists of a central vessel surrounded by tumor cells – the whole structure being contained in a cystic space often lined by flattened tumor cells. It represents an attempt to form yolk sacs. **(D)** Section of normal testicular parenchyma with higher-magnification inset (lower right; not provided by the patient described within this study).

RESULTS

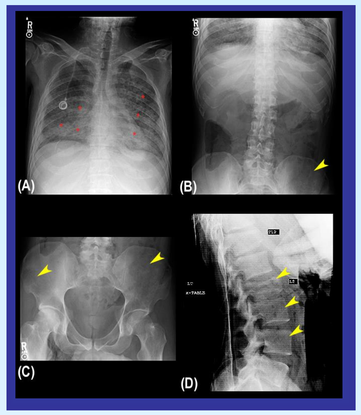

Figure 2. Plain X-Rays. Post-mortem, AP plain x-rays as shown. **(A)** AP CXR showing numerous opacities (asterisk) in the Lt and R lung fields. The dome of the diaphragm over the liver is slightly elevated, and the liver and spleen are hyper-dense with hepato- and splenomegaly. **(B)** AP Abdominoplevic flat film demonstrating heterogenous area over the vertebral bodies, and several areas of radiolucency on the ala of the right and left (more prominent, arrow) ilium. Hepatomegaly extends past R12. **(C)** AP Pelvis film clearly showing ala with increased radiolucency (arrows). **(D)** Left Lateral view of lumbar spine showing multiple areas of hypo-density in vertebral bodies (arrows) being most prominent at L2 (with compression fracture) and L3. There is also a compression fracture in T12. [Abbreviations: anterior-posterior (AP); chest x-ray (CXR); right (R); left (Lt); thoracic (T); lumbar (L).]

Figure 3. Computed Tomography. (A) COR Scout View of patient showing multiple densities in the thorax; increased density of the hepatic and splenic areas and radiolucency in the ala of the L ilium. **(B)** AX CT of Thorax at vertebral level T7 (see "A") showing multiple metastatic foci in the L and R lung fields. **(C)** AX CT of Abdomen at vertebral level T12 (see "A") showing extensive hepatomegaly the multiple tumors and invasion of tumor into vertebral body. **(D)** Contrast inverted AX CT of superior pelvic region at vertebral level S1 showing metastatic infiltration into S1 and through the L ilium. **(E)** Contrast inverted mid-SAG CT showing tumor infiltration vertebral bodies at multiple levels. [Abbreviations: Anterior (A), Axial (AX), Computed Tomography (CT), Coronal (COR), Foot (F), Head (H), left (L), Posterior (P), right (R), Sacral (S), Sagittal (SAG), Thoracic (T).]

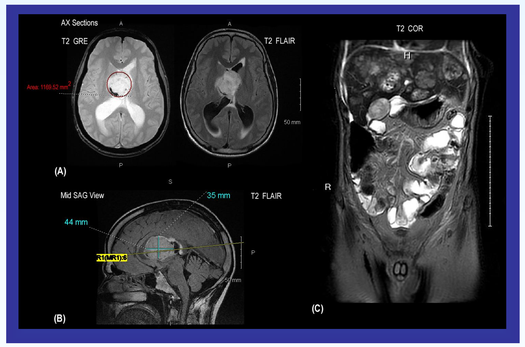

Figure 4. Magnetic Resonance Imaging. (A) T2-Wtd AX images of the brain without (GRE) and with (FLAIR) suppression of signal from cerebrospinal fluid showing centralized tumor focus with area of 1169.52 mm^2 and obstructive hydrocephalus of the lateral ventricles. **(B)** T2-Wtd Mid SAG view showing tumor with dimensions of 44 mm x 35 mm. **(C)** T2-Wtd COR abdominopelvic view with extensive hepatomegaly and liver parenchyma filled with multiple tumors of various sizes. [Abbreviations: Anterior (A), Axial (AX), Coronal (COR), Posterior (P), right (R), Sagittal (SAG), Superior (S); Weighted (Wdt).]

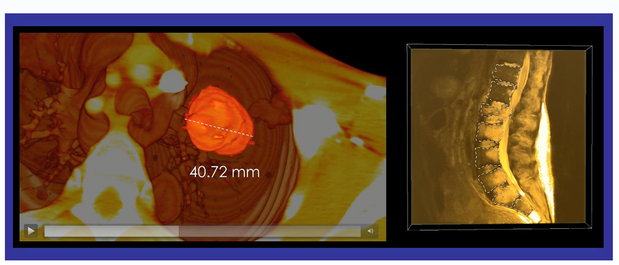

Figure 5. Radiographic 3D-Visualization. (Left Panel - Thorax and Tumors) Axial dissection with measurement of tumor masses: 40.72 mm, 45.85 mm; 36.67 mm, 32.57 mm, 10.67 mm, 10.49 mm, 15.41 mm (left lung); 31.90 mm, 28.99 mm, 6.37 mm; 7.84 mm, 76.11 mm, 67.42 mm, 4.69 mm, 8.94 mm, 5.66 mm, 9.32 mm, 10.83 mm, 10 mm and 3.26 mm (right lung). **(Right Panel - Spine Metastases)** Sagittal dissection of spine with multiple tumors (T12 - S1) and impingement on spinal cord (L2 and L3).

DISCUSSION

- TC's are increasing in incidence.
- YST originates from cells lining the yolk sac in the embryo.
- YST in pure form are rare in adults, most commonly they appear mixed with other types. The main histological feature is the presence of Schiller-Duval bodies.
- The etiology of YST is essentially unknown, however cryptorchidism is the major risk factor.
- The prognosis is favorable in children but in adults, the tumor becomes aggressive and metastasize rapidly.
- Staging of testicular cancer includes determination of the tumor (T), node (N), metastasis (M) and serum tumor markers (S).
- Metastatic routes are: hematogenous (testicular a., deferential a., cremasteric a., testicular v., pampiniform plexus, ureteral plexus, prostatic and lumbar venous plexuses); lymphogenous (pre- and para-aortic; retroperitoneal and iliac nodes); direct infiltration.
- Typical Chemotherapy treatment is BEP-Bleomycin, Etoposide, Cisplatin (typically 3 cycles).

CONCLUSIONS

- This investigation has described a case of stage III TGCT of yolk-sac type in an adult male with metastases to nodes, bone, viscera and brain. This case is interesting because **(1)** it differs from the usual TC type found in adult (vs. young) males; **(2)** it presents a histological tumor-type consistent with a pure form of YST with both glomerular and microcytic patterns and fibrosis; **(3)** it reveals the presence of a large intraventricular brain tumor, and **(4)** multiple routes of metastatic disease.
- Secondary to the worldwide increasing incidence of TC, and because surgeries can be safely combined with adjuvant therapies but have potential for significant morbidity, a multidisciplinary team with expert knowledge of anatomical patterns of metastasis and experience in treating TGCT is essential for optimal patient outcomes.

ACKNOWLEDGEMENT

Joshua G. Pate
Regina Bergner, mother of Joshua G. Pate

Methodist Hospitals Southlake Campus (Merrillville, IN)
Rocco Prosthetic and Orthotic Center (Cincinnati, OH)
Indiana University School of Medicine-Northwest (Gary, IN)
BodyViz (Clive, IA)

REFERENCES

1. TRABERT B, CJEM K. DEVESA SS, BRAY F, MCGLYNN, KA (2015) International patterns and trends in testicular cancer incidence, overall and by histological subtype, 1973-2007. Andrology, 3(1): 4-12.
2. FERLAY J, STCLIAROVA-FOUCHER E, LORTET-TICULENT J, ROSSO S, COEBERGH JWW, COMBER H, FORMAN D, BRAY F (2013) Cancer incidence and mortality patterns in Europe: Estimates for 40 countries in 2012. Eur J Cancer, 49(6): 1374-1403.
3. MCGLYNN KA, TRABERT B (2012) Adolescent and adult risk factors for testicular cancer. Nat Rev Urol, 9(6): 339-349.
4. CHIA VM, QURAISHI SM, DEVESA SS, PURDUE MP, COOK MB, MCGLYNN KA (2010) International trends in the incidence of testicular cancer, 1973–2002. Cancer Epidemiol Biomarkers Prev. 19(4): :1151–1159.
5. National Cancer Institute: PDQ® Testicular Cancer Treatment. Bethesda, MD: National Cancer Institute. Date last modified 01/26/2017. Available at: https://www.cancer.gov/types/testicular/hp/testicular-treatment-pdq#section/all Accessed 06/15/2017. https://www.cancer.gov/types/testicular/hp/testicular-treatment-pdq
6. LOTAN TA (2015) Chapter 21, The lower urinary tract and male genital system. In. Pathologic Basis of Disease, 9th Ed., Elsevier Suanders, 959-989.
7. STEVENSON SM, LOWRANCE WT (2015) Epidemiology and diagnosis of testis cancer. Urol Clin N Am, 42: 269-275.
8. SULEYMAN N, MOGHUL M, GOWRIE-MOHAN S, LANE T, VASDEV N (2016) Classification, epidemiology and therapies for testicular germ cell tumours. J Genit Syst Disor, S2(0)(2): 1-3.
9. HANNA NA, EINHORN LH (2014) Testicular cancer – discoveries and updates. N Eng J Med, 371: 2005-2016.
10. GHAZARIAN AA, TRABERT B, GRAUBARD BI, SCHWARTZ SM, ALTEKRUSE SF, MCGLYNN KA (2015) Incidence of testicular germ cell tumors among US men by census region. Cancer, 121(23): 4181-4189.
11. PETTERSSON A, RICHARDI L, NORDENSKJOLD A, KAUSER M, AKRE O (2007) Age at surgery for undescended testis and risk of testicular cancer. N Eng J Med, 356: 1835-1841.
12. FERGUSON L, AGOULNIK AI (2013) Testicular cancer and cryptorchidism. Front Endocrinol (Lausanne), 4(32): 1-9.
13. ADRA N, EINHORN LH (2017) Testicular Cancer Update. Clin Adv Hematol Onco, 15(5): 386-396.
14. FELDMAN DR, LORCH A, KRAMAR A, ALBANY C, EINHORN LH, GIANNATEMPO P, NECCHI A, FLECHON A, BOYLE H, CHUNG P, HUDDART RA, BOEKMEYER C, TRYAKIN A, SAVA T, WINQUIJST EW, DE GIORGI U, APARICIO J, SWEENEY CJ, CHON CEADERMARK G, BEYER J, POWLES T (2016) Brain metastases in patients with germ cell tumors: prognostic factors and treatment options – an analysis from the global germ cell cancer group. J Clin Oncol, 34(4): 345-351.
15. BOYLE HJ, JOUANNEAU 3, DROZ JP, FLECHON A (2013) Management of brain metastases from germ cell tumors: a single center experience. Oncology, 85(1): 21-16.

ABSTRACT

Purpose: The purpose of this investigation was to characterize an unusual case of stage III testicular germ cell tumor (TGCT) in a 31-year-old male with metastases to nodes, bone, viscera and brain, and to understand all possible routes of metastatic disease. Testicular cancer (TC) has an increasing incidence worldwide, and its etiology, risk factors and pathogenesis are not completely understood.

Methods: Medical records were reviewed, and the cadaveric specimen evaluated by physical examination and gross dissection. Paraffin embedded tissue sections of the primary tumor were stained with Hematoxylin and Eosin (H&E) for histological study. To examine metastatic spread, pre- and post-mortem digital radiologic image acquisition was done using x-ray films, and high- resolution CT Scans and MRI Scans. Image analysis, multi-planar reformatting, and three-dimensional (3-D) reconstruction were done on radiographic series.

Results: Dissection showed masses bilaterally from the apex through the lung base; masses on the internal thoracic wall, and hepatomegaly and splenomegaly with multiple tumor masses. Testicular parenchyma was composed of primitive germ cells that formed glomeruloid or embryonal-like structures, as well as areas with a micro-cystic histologic pattern and areas of fibrous dysplasia. Medical imaging 3-D video radiographic dissection was notable for a 38.45 mm diameter, mid-brain tumor; extreme hepatomegaly with numerous tumors, a large penetrating tumor of the left ilium, and multiple tumors throughout both lungs and the thoracolumbar spine (T5-S1).

Conclusion: This study provides insight into the histology and metastatic spread of TGCT that is essential for clinicians to understand in the evaluation and treatment of TC patients.

.

Talarico, Jr., E.F., **Mas, J.L.,** Jones, J.A.. (2018) A comprehensive anatomical characterization and radiographic study of stage III testicular cancer in a 31-year-old male patient. *Eur J Anat*, 22(3):241-256.

CORRESPONDENCE

Jose L. Mas, D.V.M.
Assistant Professor of Clinical Anatomy & Cell Biology
Indiana University School of Medicine - Northwest
Dunes Medical Professional Building, Room 3058, 3400 Broadway
Gary, Indiana 46408-1197 USA
TEL: 219-981-5625; FAX: 219-980-6566; Email: jlmas@iun.edu